

Effect of flow-induced exchange in hyporheic zones on longitudinal transport of solutes in streams and rivers

Anders Wörman

Department of Earth Sciences, Uppsala University, Uppsala, Sweden

Aaron I. Packman

Department of Civil Engineering, Northwestern University, Evanston, Illinois, USA

Håkan Johansson and Karin Jonsson

Department of Earth Sciences, Uppsala University, Uppsala, Sweden

Received 13 July 2001; revised 11 September 2001; accepted 18 September 2001; published 3 January 2002.

[1] Temporary storage of solutes in streams is often controlled by flow-induced uptake in hyporheic zones. This phenomenon accounts for the tails that are generally observed following the passage of a solute pulse, and such exchange is particularly important for the transport of reactive substances that can be subject to various biogeochemical processes in the subsurface. Advective pumping, induced by streamflow over an irregular permeable bed, leads to a distribution of pore water flow paths in the streambed and a corresponding distribution of subsurface solute residence times. This paper describes a modeling framework that couples longitudinal solute transport in streams with solute advection along a continuous distribution of hyporheic flow paths. Moment methods are used to calculate the shape of solute breakthrough curves in the stream based on various representations of hyporheic exchange, including both advective pumping and several idealized formulations. Basic hydrodynamic principles are used to derive the distribution of solute residence times due to pumping. The model provides an accurate representation of the breakthrough curves of tritium along a 30 km reach of Säva Brook in Uppland County in Sweden. Both hydrodynamic theory for pumping exchange and pore water samples obtained from the bed during the tracer experiment suggest that the residence time for solutes in the hyporheic zone is characterized by a log normal probability density function. Closed-form solutions of the central temporal moments of solute breakthrough curves in the stream reveal a significant similarity between this new model and existing models of hyporheic exchange, including the Transient Storage Model. The new model is advantageous because its fundamentally derived exchange parameters can be expressed as functions of basic hydrodynamic quantities, which allows the model results to be generalized to conditions beyond those directly observed during tracer experiments. The utility of this approach is demonstrated by using the pumping theory to relate the spatial variation of hyporheic exchange rate along Säva Brook with the local Froude number, hydraulic conductivity and water depth. *INDEX TERMS:* 1871 Hydrology: Surface water quality, 1806 Hydrology: Chemistry of fresh water, 3210 Mathematical Geophysics: Modeling; *KEYWORDS:* hyporheic zone, streams, solute transport, tracer test, temporal moments, pumping exchange

1. Introduction

[2] Transport of reactive solutes in streams is controlled to a great extent by the combination of exchange with hyporheic zones or adjacent wetland areas, sorption on to particulate matter, and various biogeochemical reactions [Kim *et al.*, 1992; Runkel and Bencala, 1995; Wood and Baptista, 1993]. Thus it is critical to understand the mechanisms of hyporheic exchange in order to analyze the transport and fate of environmentally important substances such as nutrients, carbon, and toxic contaminants in watersheds.

[3] Exchange with the hyporheic zone has been represented in several different ways, but the most common goal of modeling efforts has been to reproduce the observed longitudinal and temporal variation of solute concentrations in streams and rivers

[Packman and Bencala, 1999]. Thackston and Schnelle [1970], Bencala and Walters [1983] and Runkel *et al.* [1996a, 1996b] used first-order mass transfer relationships to describe solute exchange between streams and transient storage zones. The first-order mass transfer relationship is a parameterization of all mechanisms governing solute mixing in the hyporheic zone. Exchange with the hyporheic zone has also been represented as a diffusive process [Richardson and Parr, 1988; Wörman, 1998].

[4] Jackman *et al.* [1984] and Wörman [2000] provide formal comparisons of different parameterizations of the solute exchange with the hyporheic zone, and these studies found small but definite differences in the various model characteristics. The diffusive-type exchange relationship retains certain hydro-mechanical characteristics of the mixing process that are omitted from the first-order mass transfer model, such as a variable concentration with depth and a gradient-controlled transport rate. Nonetheless, the diffusive exchange model is known to be a considerable abstraction of

reality, as effective diffusive exchange coefficients have often been found to be orders of magnitude higher than fundamental molecular diffusion coefficients.

[5] Both the diffusive and the first-order exchange models have been successfully used to interpret longitudinal solute transport in streams [Bencala and Walters, 1983; Choi *et al.*, 2000; Wörman *et al.*, 1998; Jonsson and Wörman, 2000; Johansson *et al.*, 2000]. Despite their success, both models represent rather crude simplifications of true hyporheic mixing behavior. Essentially, the diffusive and mass transfer models simply provide a convenient mathematical framework for analysis of solute breakthrough curves, but do not realistically represent the physics of the exchange process. This inconsistency prohibits independent estimations of the mixing coefficients in terms of bed properties and streamflow conditions. Instead, estimation of exchange parameters relies on costly, time consuming, and reach-specific measurements in streams. In addition, the use of empirical model parameters makes it very difficult to apply the model for conditions other than those for which the exchange parameters were experimentally obtained.

[6] It is now known that transient storage is largely controlled by advection into and out of the hyporheic zone, as discussed by Thibodeaux and Boyle [1987], Elliott [1990], Harvey and Bencala [1993], Huettel *et al.* [1996], Elliott and Brooks [1997a], Hutchinson and Webster [1998], Packman [1999], and Packman and Brooks [2001]. Advective exchange between the stream and the hyporheic zone can control the transport of both dissolved species and colloidal matter [Packman *et al.*, 1997, 2000a]. Fundamental exchange models based on the pumping process have successfully predicted the hyporheic exchange observed in laboratory flume experiments, such as those of Elliott and Brooks [1997b] and Packman *et al.* [2000b]. However, the fundamental advective exchange models have only been applied to a very limited number of natural rivers [Rutherford *et al.*, 1993, 1995], in large part because direct application of these models requires extensive site characterization and no methodology exists to formally derive simpler models that can be applied to field cases.

[7] The purpose of this study is to couple a physically based representation of flow-induced uptake in the hyporheic zone with a model for the longitudinal in-stream solute transport. Hyporheic exchange will be calculated based on the theory of Packman *et al.* [2000a]. Moment methods [Schmid, 1995; Wörman, 2000] will be used to link the residence times of solutes in the hyporheic zone with longitudinal solute transport in the stream. The resulting model will be evaluated using results from the field tracer experiment of Johansson *et al.* [2000] and K. Jonsson *et al.* (Uncertainty of retention of solutes in hyporheic zones evaluated from stream tracer injections, submitted to *Water Resources Research*, 2001, hereinafter referred to as Jonsson *et al.*, submitted manuscript, 2001). A combination of observations of solute concentrations in the stream water and the streambed will be used to provide a reliable basis for evaluation of the new model.

[8] By considering more accurately the actual mixing process in the hyporheic zone, the new model allows generalization of results from individual stream tracer experiments. This is an important objective in order to model exchange under various discharge conditions and in stream reaches outside the scope of tracer experiments. In addition, the model framework presented here can provide the basis for the prediction of hyporheic exchange from fundamental physical parameters. We believe that this approach can serve as the foundation of new efforts to model

hyporheic exchange based on fundamental analysis of the underlying hydrodynamic transport processes.

2. Theory of Solute Transport in Streams With Hyporheic Exchange

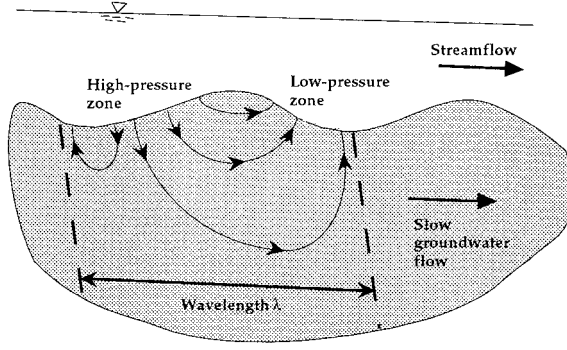
2.1. Residence Time Model for Hyporheic Exchange

[9] Hyporheic exchange is commonly formulated as a first-order mass transfer with the exchange defined by two parameters: an exchange coefficient and a storage zone depth or area [Bencala and Walters, 1983; Jackman *et al.*, 1984]. This formulation, known as the Transient Storage Model (TSM), yields an exponential probability density function of the return times of the exchanged solute mass from the storage zone and conveniently represents the “tailing” in concentration seen after the passage of a solute pulse. The mass transfer exchange rate coefficient (units of inverse time) represents the timescale of the transient storage. However, since there is often natural variability in hyporheic exchange, under some conditions the model must include multiple exchange rates [Choi *et al.*, 2000].

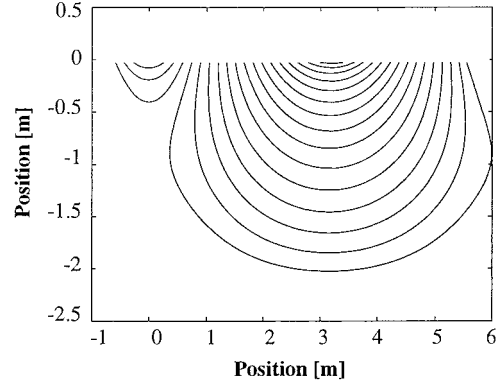
[10] In order to develop a more realistic model for hyporheic transient storage, we suggest here a formulation for the residence time of solutes in the hyporheic zone that is based on knowledge of hyporheic flow dynamics. The residence time distribution will first be derived from hydrodynamic principles (in section 2), then used to calculate the moments of a solute pulse passing in the overlying water column (section 3), and evaluated using the results of tracer tests conducted in a small stream (section 4). Different residence time distributions will be used, one of which is the exponential associated with the TSM, and their implications will be compared with that derived from the hydrodynamic principles applied here.

[11] It is worthwhile to test different residence time distributions because several conditions can induce a flow of water and solute elements between the stream and the hyporheic zone, and these various processes are expected to produce different distributions of subsurface retention times. For instance, exchange can occur in a meandering river that has different flow directions in relation to the direction of the groundwater flow [Wroblicky *et al.*, 1998] and in streams with spatially varying slope [Harvey and Bencala, 1993; Castro and Hornberger, 1991]. A flow can also be induced in the hyporheic zone due to the mechanics of streamflow over irregularities on the bed surface. Characteristic topographical features known as bed forms develop naturally due to streamflow over a loose sediment bed [Vanoni, 1975; Raudkivi, 1998]. Additional irregularities can be formed by biotic processes [Huettel *et al.*, 1996] or by obstacles like stones or tree branches [Hutchinson and Webster, 1998]. An obstruction in a turbulent flow will generally produce a high-pressure region on the upstream side of the obstruction and a low-pressure recirculation region downstream. Hence water and solutes enter the bed at high-pressure zones on bed forms and exit at low-pressure zones as depicted in Figure 1. This phenomenon has been termed “pumping.”

[12] The induced hyporheic flows discussed above show great similarity in that they are defined by a distribution of travel times that are caused by a spatially periodic variation of hydraulic head along the stream boundary. The subsurface flow follows the continuity equation and, when the permeability of the hyporheic zone is sufficiently low, Darcy’s law. In principle, these equations can be solved using the exact boundary conditions of specific cases. A useful general approximation, however, is to assume that the bed surface is flat, the sediment is homogeneous, and there is a sinusoidal distribution of pressure head along the bed surface. Elliott [1990], Eylers *et al.* [1995], Elliott and Brooks [1997a, 1997b], and Pack-



Pumping exchange in bed with uneven bed surface



Sinusoidal pressure variation along flat bed surface

Figure 1. Streamlines in a streambed due to periodic pressure variations along an uneven bed surface. The right-hand side diagram shows streamlines derived using the flat bed approximation, following the theory of *Packman et al.* [2000a]. The relative depth of the hyporheic zone $d_b/\lambda = 0.4$, and the longitudinal groundwater velocity $u_{adv}^* = 0.4 u^*$ ($x = 0, z = 0$).

man et al. [2000a, 2000b] have presented a theory for the pumping flow field using a flat bed approximation that will be discussed further in section 2.2. The right-hand diagram in Figure 1 shows the streamlines determined by calculating trajectories of inert particles in the bed under the imposed head distribution and a superimposed longitudinal groundwater flow, with an impermeable surface limiting the downward extension of the hyporheic zone.

[13] Advective pumping exchange is characterized by a pore water velocity field $V(x, y)$. Here we denote the infiltration velocity into the bed in the direction of the streamlines by $V_z(T, \tau)|_{\tau=0}$ (m s^{-1}) and the exfiltration velocity out of the bed in the direction of the streamlines by $V_z(T, \tau)|_{\tau=T}$ (m s^{-1}), where z denotes a curve-linear coordinate along the hyporheic flow path. These velocities are defined as Darcy velocities (the product of the pore water velocity and bed porosity), and the exfiltration is defined by a residence time, τ [s] ($0 < \tau < T$), where T is the total residence time due to transport along an individual exchange flow path. The dissolved solute exchange rate per unit bed area is the product of the component of the exchange velocity perpendicular to the bed surface and the dissolved solute concentration in the stream water, c_d (kg m^{-3}).

[14] Using this framework, the net solute mass flux ($\text{kg m}^{-3} \text{s}^{-1}$) in the dissolved phase in the stream water can be found by integrating over the distribution of transport pathways:

$$J_s = \frac{1}{2} \int_0^\infty f(T) \frac{P}{A} \xi \cdot (-V_z(\tau, T)|_{\tau=0} c_d + (V_z(\tau, T)g_d)|_{\tau=T}) dT, \quad (1)$$

where g is solute mass per unit volume of water in the hyporheic zone (kg m^{-3}), $f(T)$ is the probability density function (PDF) of T weighted by the velocity component normal to the bed surface, V_n , P is the wetted perimeter, A is the cross-sectional area of the stream, and ξ is an area reduction factor equal to V_n/V_z that accounts for the fact that the streamlines are not necessarily always perpendicular to the bed surface. The introduction of V_z and ξ simplifies the forthcoming analysis because $\int_0^\infty V_n(T)/V_z(T)f(T)dT$ has been found to be close to constant and V_z varies only little along the bed (compare section 2.2). Hence both V_z and ξ are treated as constants. For the sake of simplicity, the averaging operation $\int_0^\infty f(T) \dots dT$ will subsequently be denoted by brackets $\langle \dots \rangle$. The first term of the right-hand side of (1) is due to the flow of solute into the bed, and the second term

represents the flow of solute out of the bed. The factor 1/2 in the flux expression is introduced because half of the bed is subjected to infiltration and the other half to exfiltration. The term $V_z/2$ can be interpreted as an effective exchange velocity.

[15] Solute transport in the stream can be coupled with the hyporheic exchange flux by writing a mass balance for solute in the stream:

$$\frac{\partial c_d}{\partial t} + \frac{1}{A_T} \frac{\partial(AUc_d)}{\partial x} - E \frac{\partial^2 c_d}{\partial x^2} = J_s, \quad (2)$$

where A_T (m^2) is the cross-sectional area of the main stream including side pockets, A is the cross-sectional area of the main stream excluding side pockets, U is the flow velocity in the main stream (m s^{-1}) ($Q = UA$), Q is the discharge ($\text{m}^3 \text{s}^{-1}$), and E is the main stream dispersion coefficient ($\text{m}^2 \text{s}^{-1}$). The effective flow velocity in the main stream channel corrected for side pockets with stagnant water is given by $U_e = Q/A_T$ [Wörman, 1998]

[16] Equations (1) and (2) allow solute breakthrough curves in the stream to be calculated from in-stream transport parameters and the residence time distribution of solutes in the subsurface. The residence time distribution will be evaluated from fundamental principles in section 2.2, their impact on the longitudinal solute transport is analyzed in section 3 and section 4 contains a comparison with experimental results. The overall hyporheic exchange model, essentially defined by (1) in combination with (2), will be subsequently referred to as the Advective-Storage-Path Model (ASP model).

2.2. Residence Time PDF Derived From Hydrodynamic Principles

[17] The pumping process described in section 2.1 can be analyzed using hydromechanics to describe the residence time distribution for hyporheic exchange locally in a streambed. The model framework used for these particular analyses will be referred to as the ‘‘pumping exchange model’’ and can be used to derive specific information of the ASP model that represents also the transport along the stream. The approximations of a flat surface and sinusoidal pressure variation, while not necessarily strictly applicable to all cases, can be used to derive important insights into the relationship between state variables, exchange velocities, and

the residence time distribution. If we use the scale variables suggested by *Elliott and Brooks* [1997a] and *Packman et al.* [2000a] whereby the dimensionless velocity $V_z^* = (V_z \lambda) / (2 \pi K h_m)$, the dimensionless time $t^* = 4 \pi^2 (t K h_m) / \lambda^2$, and the streambed depth is scaled with the bed form wavelength, we can express the flow field as a unique function of two parameters, d_b / λ and u_{adv}^* / V_z^* ($x = 0, z = 0$), where λ is the wavelength of the pumping pressure distribution, K is the hydraulic conductivity (m s^{-1}) h_m is the maximum pressure head due to pumping, d_b is the mean depth of the hyporheic zone (corresponding with the location of an impermeable boundary), and u_{adv} is the longitudinal velocity of the underlying groundwater flow.

[18] By employing numerical “particle tracking” simulations and the pumping exchange model, we calculated the probability density function for the residence time distribution (T-PDF) as a function of d_b / λ . This result is shown in Figure 2. For typical stream conditions the longitudinal groundwater flow induced by the mean stream slope does not have a significant impact on the residence times [Packman et al., 2000a]. As can be seen in Figure 2, longer residence times dominate for hyporheic zones of increasing depth until an asymptote is reached for $d_b / \lambda > \sim 1.0$. This is because a shallow impermeable layer restricts the hyporheic flow to a region near the stream-subsurface interface, where the pore water velocities are higher. A good approximation for the residence times in the range $0.3 < d_b / \lambda < 1.0$ is given by

$$\langle T^* \rangle = 4\pi^2 \frac{\langle T \rangle K h_m}{\lambda^2} = 21 d_b / \lambda. \quad (3)$$

For larger values of d_b / λ the dimensionless residence time is approximately constant, $\langle T^* \rangle \approx 25$. The exchange velocity normalized in the form $E[V_z]_{z=0} / \max[V_z]_{z=0}$ was found to be practically constant along the bed; for stagnant groundwater its value varied from 0.84 when $d_b / \lambda = 0.1$ up to 0.98 when $d_b / \lambda = 2.0$. A good approximation of the exchange velocity is given by

$$\langle V_z \rangle_{z=0} = (2\pi K h_m) / \lambda. \quad (4)$$

The corresponding area reduction factor ξ is evaluated as $\int_0^\infty V_m / V_z f(T) dT$ and was found to be fairly constant $\xi \approx 0.79$ for $0.3 < d_b / \lambda$.

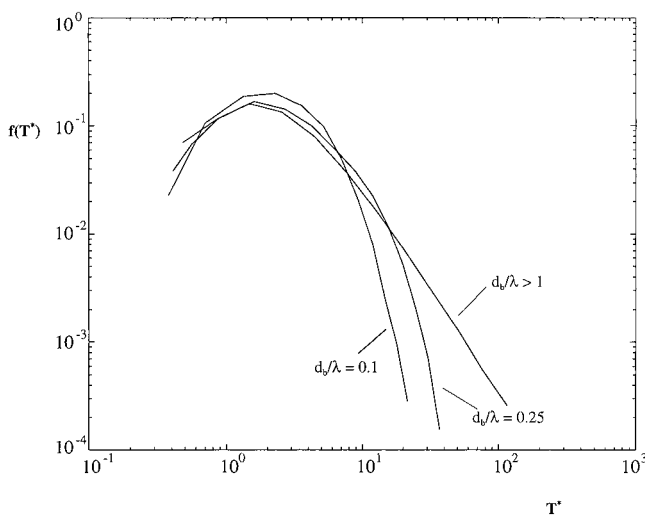


Figure 2. Residence time PDFs associated with the flat boundary approximation and a sinusoidal pressure variation. The probability density function is weighted by discharge.

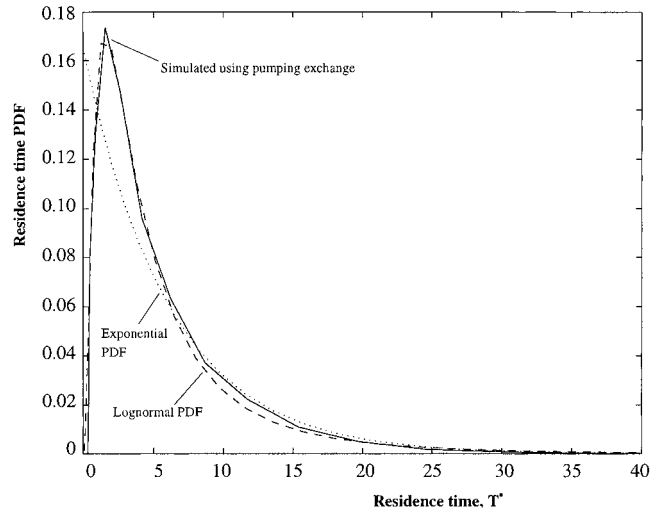


Figure 3. Residence time PDF simulated by means of the pumping exchange model with the flat boundary approximation and sinusoidal pressure variation along the bed and $d_b / \lambda = 0.25$. Two distribution functions are included as comparison using the following values: $\langle T^* \rangle = 6.05$, $\alpha = 1.35$, and $\beta = 0.947$, where α and β are the coefficients of the lognormal PDF defined in Table 1.

[19] The variation of the velocity along the travel paths was quantified in terms of $E[V_z]_{mid} / V_z|_{z=0}$, where the subscript “mid” indicates a position exactly in the middle of the travel path. If the groundwater advection is zero, this ratio assumes a lowest value slightly below 0.7 for $d_b / \lambda > 0.5$ and approaches unity as d_b / λ decreases below 0.5. Since the velocity V_z is fairly constant both along the bed and along the travel paths, it will be taken as a constant in the following derivation.

[20] The residence time PDF of the pumping exchange model is very closely log normal as shown in Figure 3, but an exponential function provides a fair approximation. This indicates that the Transient Storage Model can often be expected to provide a reasonable representation of the pumping process. The best fit of the log normal PDF with $d_b / \lambda = 0.25$ was obtained for $\alpha = 1.35$ and $\beta = 0.947$ (definitions can be found in Table 1). The values of α and β change with d_b / λ , and this motivates that these parameters are obtained by fitting the model versus solute concentration data.

[21] The applicability of the pumping exchange model is also limited by the simplifications on which it is based, i.e., a flat bed with a harmonic pressure variation. We can imagine the wave crests of the sediment surface conducting larger flows than if these parts of the bed were flat (compare Figure 1). Since the wave crests contain the lower quartile of the residence times, we can expect that shorter residence times will be relatively more important in most real streams (relative to the PDFs shown in Figure 3). This effect has been inferred from flume experiments with relatively large, sharp bed forms (A. Marion et al., Penetration of passive solutes into a streambed, submitted to *Water Resources Research*, 2001, hereinafter referred to as Marion et al., submitted manuscript, 2001). Thus, in section 4, we will examine the hyporheic residence times observed following injection of a tracer into a small stream, and compare these with the result predicted by the pumping exchange model. The residence time PDF will be evaluated using experimental data from the analysis of both stream water and pore water extracted from the hyporheic zone.

Table 1. Coefficients of the Central Temporal Moments of the Residence Time PDF in the Flowing Water Resulting From Different T-PDFs

Type of T-PDF	Degrees of Freedom of PDF	Coefficients in the Central Temporal Moments of the Solute Breakthrough Curve
Dirac delta distribution (single hyporheic flow path): $f(T) = \delta(T - \langle T \rangle)$; $T \in [-\infty, \infty]$	one degree defined by mean value, $\sigma_T^2 = 0$	$a = 1$; $b = 1$; $c = 1$
Uniform distribution: $f(T) = \frac{1}{2\langle T \rangle}$; $T \in [0, 2\langle T \rangle]$	one degree defined by mean value, $\sigma_T^2 = \langle T \rangle^2/3$	$a = 4/3$; $b = 2$; $c = 16/5$
Exponential distribution (Transient Storage Model): $f(T) = 1/\langle T \rangle e^{-T/\langle T \rangle}$; $T \in [0, \infty]$	one degree defined by mean value, $\sigma_T^2 = \langle T \rangle^2$	$a = 2$; $b = 6$; $c = 24$
Lognormal distribution (pumping model and others): $f(T) = \frac{1}{\beta T \sqrt{2\pi}} e^{-(\ln T - \alpha)^2 / (2\beta^2)}$; $T \in [0, \infty]$ $E[T] = \langle T \rangle = e^{\alpha + \beta^2/2}$ $\sigma_T^2 / \langle T \rangle^2 = (e^{\beta^2} - 1)$	two degrees defined by mean value and variance	$a = \exp(\beta^2)$; $b = \exp(3\beta^2)$; $c = \exp(6\beta^2)$

2.3. Solution to ASP Model With Transport Equations for Solute in Hyporheic Zone

[22] We have introduced the residence time distribution of solutes in the hyporheic zone, but this does not uniquely define the rate of solute mass exchange between the stream and the hyporheic zone. The exchange rate depends also on the accumulation capacity of the hyporheic zone [e.g., *Harvey et al.*, 1996] or, as an alternative, the magnitude of the hyporheic exchange velocity. The exchange velocity is introduced in (1), and use of this property leads directly to the transport equations of the hyporheic zone. This is essential in order to facilitate future extensions to cope with reactive substances and variety of different early diagenetic processes like sorption kinetics, bioturbation, etceteras [*Comans and Hockley*, 1992; *Smith and Comans*, 1996; *Meili and Wörman*, 1996]. For a nonreactive solute, mass conservation arguments yield

$$\frac{\partial g_d n}{\partial t} + \frac{1}{A_t} \frac{\partial A_t V_z g_d}{\partial z} = 0, \quad (5)$$

where n is the porosity, $1/A_t \partial A_t / \partial x$ reflects a relative divergence (m^{-1}) of an imaginary flow tube with a cross-sectional area $A_t (\text{m}^2)$, and g is dissolved solute mass in the bed per unit volume of pore water. As boundary condition at inflow locations, the dissolved phase concentration is continuous at the streambed interface:

$$g_d(z = 0, t) = c_d(x, t). \quad (6)$$

[23] Consideration of advective transport along hyporheic flow paths allows us to analyze the effect of different types of T-PDFs on solute breakthrough in the stream. Illustrative results are shown here, and the solution procedure is described in Appendix A. Figure 4 shows that when we use only a single residence time (Dirac-type T-PDF), the solute that enters the hyporheic zone will travel along the hyporheic travel path for a definite time $\langle T \rangle$ and give rise to a series of peaks that are time-lagged with a period $\langle T \rangle$. The multiple peaks become smoothed out when we introduce a uniform and an exponential distribution of travel times, respectively, as shown by the dashed and the dashed-dotted curves. Consequently, the solute breakthrough in the stream depends markedly on the form of the T-PDF for hyporheic exchange. Conversely, observed breakthrough curves can be used to derive information about the residence time

distribution of solutes in the hyporheic zone and the underlying exchange processes.

3. Closed-Form Solutions for the Central Temporal Moments of Breakthrough Curves for Downstream Solute Transport

[24] The net downstream transport of a solute pulse can be represented in terms of the central temporal moments of the resulting solute breakthrough curve. The central temporal moments of the distribution change over time due to processes such as in-stream dispersion, dead zone mixing, and hyporheic exchange. Essentially, the ASP model calculates the distribution of solute mass in the stream based on in-stream transport and the residence time of solute mass in the hyporheic zone. Various formulations of the hyporheic residence time PDF can be used to yield different predictions of

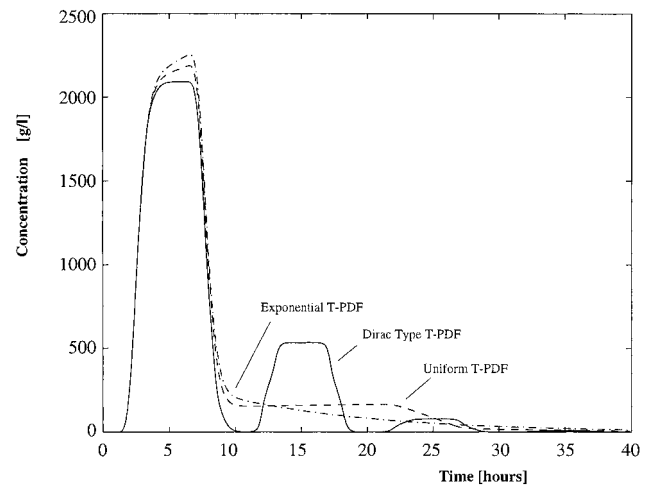


Figure 4. Simulated solute breakthrough curves for different residence time PDFs. The upstream boundary condition was a short pulse released at $t = 0$. The breakthrough indicated by the solid curve was obtained for a single path, i.e., $f(T) = \delta(T - \langle T \rangle)$, and shows a series of decaying peaks time lagged by $\langle T \rangle$, where δ is the Dirac delta function. By introducing a distribution of residence times and path lengths, the curve is smoothed out. The following representative parameter values were applied: $x = 1000$ m, $U_e = 0.105$ m s $^{-1}$, $E = 3$ m 2 s $^{-1}$, $V_z = 10 \times 10^{-6}$ m s $^{-1}$, $\langle T \rangle = 35,000$ s, and $h = 0.35$ m.

downstream solute transport. In addition, the central temporal moments of the solute pulse can be used to make a formal comparison of the ASP model with other hyporheic exchange models.

[25] To simplify the derivation of the moment equations, we assume that the dispersion in the main stream channel is negligible (i.e. $E = 0$) compared to the dispersion caused by the transient storage. This is a justifiable assumption for a sufficiently large modified Damköhler number, which is the case in the tracer experiments discussed in section 4 [Wörman, 2000; Jonsson and Wörman, 2000]. After lengthy derivations based on (1), (2), (5), and (6), assuming $E = 0$, assuming a unit pulse at the upstream boundary with constant strength and a finite duration $\Delta(s)$, the following expressions are obtained (Appendix A)

$$\mu_t = \frac{x}{Q/A_T} (1 + \langle F \rangle) + \frac{\Delta}{2} \quad (7)$$

$$\sigma_t^2 = \frac{x}{Q/A_T} \langle F T \rangle + \frac{\Delta^2}{12} \quad (8)$$

$$S_t = \frac{x}{Q/A_T} \langle F T^2 \rangle \quad (9)$$

$$K_t = \frac{x}{Q/A_T} \langle F T^3 \rangle + 3 \left(\frac{x}{Q/A_T} \right)^2 \langle F T \rangle^2 + \frac{\sigma_t^2 (\Delta = 0) \Delta^2}{2} + \frac{\Delta^4}{80}, \quad (10)$$

where $F = [1/2 (\xi P V_z T)/A]$. The moments are μ_t equal to expected value of solute residence in the stream(s), σ_t^2 equal to variance of the solute breakthrough curve(s), S_t equal to Skewness of the solute breakthrough curve(s), and K_t equal to Kurtosis of the solute breakthrough curve(s). The corresponding expressions for a unit Dirac pulse are obtained by letting the duration of the pulse be zero, i.e., $\Delta = 0$.

[26] The effect of hyporheic exchange appears in the parameters F and T . The parameter F can be seen as a hydro-mechanical retardation factor due to retention of the solute in the hyporheic zone, which reflects the size ratio between the hyporheic zone, $V_z T$, and the stream, A/P . Note that $V_z T$ is not a unique geometric property of the hyporheic zone because both V_z and T change with streamflow condition. When F is zero, the propagation velocity of the pulse is the same as the stream velocity $U_e = Q/A_T$, but the effective solute velocity decreases as F increases. The temporal moments scale with the residence time of solutes in the hyporheic zone, or equivalently with the distribution of travel times along hyporheic flow paths. For instance, the variance of the solute breakthrough curves are proportional to the product of the advective transport time, $x/(Q/A_T)$, and T . Equations (7)–(10) have exactly the same form as the corresponding expressions derived by Wörman [2000] for three other alternative hyporheic exchange models. This suggests that parameters of different models can readily be related quantitatively. In particular, the mean residence time can be expressed in terms of the exchange rate α_{st} (s^{-1}), and the hyporheic storage area A_s (m^2) used to parameterize the Transient Storage Model:

$$\langle T \rangle = (1/\alpha_{st}) A_s / A. \quad (11)$$

From this expression it is clear that the parameter $(1/\alpha_{st}) A_s / A$, evaluated in many field experiments, exactly defines the mean residence time of the solute in the hyporheic zone. The expected

residence time for solutes in the hyporheic zone has been investigated in many field studies and found to vary in a wide range [Kim et al., 1992; Czernuszenko et al., 1998; Harvey and Fuller, 1998; Wörman, 2000; Seo and Cheong, 2001; Fernald et al., 2001].

[27] Since the averaging $\langle \dots \rangle$ defines an integration over T and the central temporal moments of the residence time PDF contains various orders of T (i.e., T , T^2 , T^3 , and T^4), the averaging operation involves different orders of the moments of the T-PDF. Hence different forms of the T-PDF give different expressions for the central temporal moments. Generally, the moments can be expressed as

$$\mu_t = \frac{x}{Q/A_T} (1 + F(\langle T \rangle)) + \frac{\Delta}{2} \quad (12)$$

$$\sigma_t^2 = a \frac{x}{Q/A_T} F(\langle T \rangle) \langle T \rangle + \frac{\Delta^2}{12} \quad (13)$$

$$S_t = b \frac{x}{Q/A_T} F(\langle T \rangle) \langle T \rangle^2 \quad (14)$$

$$K_t = c \frac{x}{Q/A_T} F(\langle T \rangle) \langle T \rangle^3 + 3a^2 \left(\frac{x}{Q/A_T} \right)^2 \cdot F(\langle T \rangle) \langle T \rangle^2 + \frac{\sigma_t^2 (\Delta = 0) \Delta^2}{2} + \frac{\Delta^4}{80}, \quad (15)$$

where $F(\langle T \rangle) = [1/2 P \xi V_z \langle T \rangle / A]$ and a , b , and c are coefficients that depend on the form of the T-PDF. The simplest case is obtained when there is only a single travel path, which corresponds to $f(T) = \delta(T - \langle T \rangle)$; $T \in [-\infty, \infty]$ where δ is the Dirac Delta function. For a Dirac delta distribution $a = b = c = 1$.

[28] In Table 1 the coefficients a , b , and c are presented also for uniform, exponential, and lognormal T-PDFs. The uniform and exponential PDFs have only one degree of freedom since they are both fully defined in terms of the expected value $\langle T \rangle$. As mentioned previously, the first-order mass transfer function used in the Transient Storage Model is equivalent to an exponential PDF. Wörman [2000] previously derived the coefficients associated with the Transient Storage Model.

[29] The lognormal distribution is defined by two coefficients, α and β (Table 1) that reflect the mean and the variance of T , respectively. By including an additional degree of freedom in the T-PDF, we can control the coefficients a , b , and c by adjusting the variance parameter β . If the variance of T is zero, $\beta = 0$, and we obtain a Dirac delta distribution with $a = b = c = 1$. As β increases, the coefficients increase according to Table 1, and as a consequence, the coefficient of skewness and relative skewness, S_t/σ_t^3 , also increases (as factors of $\exp(\beta^2)$ and $\exp(1.5 \beta^2)$). According to the pumping exchange model with homogeneous hydraulic conductivity, the value of β increases from about 0.95 when the relative depth of the hyporheic zone $d_b/\lambda = 0.25$ up to 1.9 when $d_b/\lambda > 1$ (in both cases $\alpha \approx 1.35$).

4. Evaluation of the ASP Model Using Observations From Stream Tracer Experiments

4.1. Säva Brook Experiment 1998

[30] The ASP model was evaluated using data obtained from a tracer experiment performed in Säva Brook in Uppland County in Sweden using tritium as a conservative tracer. The experimental results were reported by Johansson et al. [2000] and full details of

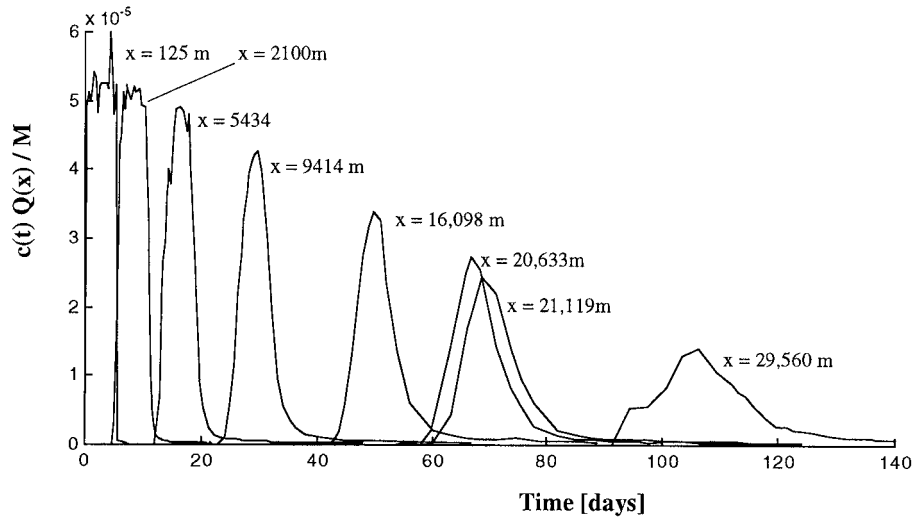


Figure 5. Breakthrough curves for tritium ($^3\text{H}_2\text{O}$) in the Säva Brook Experiment 1998. The curves are normalized in the form of temporal PDFs using the water discharge Q and total injected solute mass M . See Appendix A for mathematical details on this normalization (data after Jonsson et al. (submitted manuscript, 2001)).

the experiment are given by Jonsson et al. submitted manuscript, (2001). In the experiment both a sorbing tracer, chromium, $^{51}\text{Cr}(\text{III})$ introduced as a chromium chloride solution and a conservative tracer, tritium, $^3\text{H}_2\text{O}$, were injected simultaneously for 5.3 hours, but here we will focus on the conservative tracer as an indicator of the hydraulic mixing mechanisms in the hyporheic zone.

[31] Tritium concentrations were measured at eight stations along nearly 30 km of the Brook. These results are reported as normalized breakthrough curves (PDFs) in Figure 5. Water depth and discharge, Q ($\text{m}^3 \text{s}^{-1}$), were monitored during the experiment and found to be fairly constant, with a slight decrease observed during the course of the experiment. The discharge increased by a factor of 4.85 along the study reach to $\sim 490 \text{ L s}^{-1}$ at the downstream section. The hydraulic conductivity of the bed sediments and the channel geometry were measured with sufficient

frequency to allow evaluation of mean values in each reach with an accuracy of $\pm 20\%$ on a 95% confidence level (using the t distribution). This required extensive investigations of these properties in about 85 cross sections arbitrarily selected along the brook. The measured cross sections were equally spaced between solute measuring stations. The hydraulic conductivity was measured using a simple slug test [Freeze and Cherry, 1979] at two depths (3 and 7 cm) and in 4–5 verticals across the stream. Theoretical analyses and practical tests indicated that the sediment-water interface has a negligible effect on the slug test even at a depth of 3 cm due to the use of a small injection surface (a cylinder 12 mm in diameter and 10 mm in height). Since the available pumping exchange model assumes a constant conductivity in the sediments, we obtained representative mean values for the hyporheic zone by taking a weighed average of $K_{\text{mean}} = 0.3 K_{7\text{cm}} + 0.7 K_{3\text{cm}}$, where $K_{7\text{cm}}$ and $K_{3\text{cm}}$ indicate the results obtained

Table 2. Parameter Values Used to Evaluate the Breakthrough Curves of $^3\text{H}_2\text{O}$ in the Säva Brook Experiment 1998 by Means of the ASP model

Subreach, m	Description	Evaluation Method							
		Observations				Optimization Based on Central Temporal Moments of Tritium Breakthrough			
		θ , m^{-1}	A/P , m	h , m	Slope, 10^{-4}	K , m s^{-1}	U_e , m s^{-1}	$\langle T \rangle$, s	$\xi(V_2)/2$, m s^{-1}
0–125	coniferous forest, stream with debris and boulders
125–2,100	coniferous forest and some agriculture, some debris	4.3×10^{-5}	0.26	0.32	15.8	9.95×10^{-4}	0.105	10,325	1.27×10^{-6}
2,100–5,434	meandering stream, agriculture with macrophyte patches	4.44×10^{-4}	0.33	0.40	10.9	8.82×10^{-4}	0.121	22,355	3.73×10^{-6}
5,434–9,414	meandering stream, agriculture with macrophyte patches	4.31×10^{-5}	0.77	1.1	15.2	8.75×10^{-4}	0.088	26,180	3.96×10^{-6}
9,414–16,098	meandering stream, agriculture with macrophyte patches	3.89×10^{-5}	0.58	0.78	12.1	7.00×10^{-4}	0.093	15,266	5.90×10^{-6}
16,098–20,633	meandering stream, agriculture with macrophyte patches	7.05×10^{-6}	0.90	1.32	9.89	8.75×10^{-4}	0.076	40,750	1.42×10^{-6}
20,633–21,119	dense macrophyte patch	8.1×10^{-5}	0.044	42,607	2.94×10^{-6}
21,119–29,560	meandering stream, agriculture with macrophyte patches	1.86×10^{-5}	0.97	1.36	15.9	10.0×10^{-4}	0.0689	48,467	4.06×10^{-6}

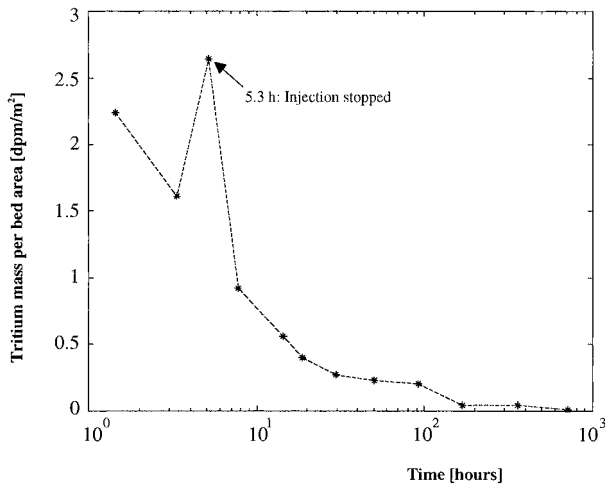


Figure 6. Tritium mass in streambed sediment at section $x = 125$ m in the Säva Brook Experiment, 1998. Each data point represents averages of 6–7 sediment cores taken to a depth up to 21 cm at station A (data after Jonsson et al. (submitted manuscript, 2001)).

from slug tests at 7 and 3 cm depth, respectively. This weighted average reflects the fact that pumping exchange is biased toward the near-surface flow paths. The values of hydraulic conductivity listed in Table 2 are these mean values.

[32] Evaluation of the tritium inventory in the stream sediments, obtained from sampling 6–7 sediment cores of the bed sediment, indicates that more than 90% of the observed transient storage occurred due to exchange with the streambed. Sediment cores of

up to 21 cm length were obtained, which is sufficiently deep to capture the entire solute concentration profile in the bed. Figure 6 shows that considerable tritium mass remained in the bed for several weeks after the injection. Obviously, the time required to flush tritium from the bed is much longer than the uptake period. For such conditions and on the assumption that advection dominates the transport in the bed, the residence time of the solute in the bed weighted by discharge can be shown to be proportional to the time rate of change of the solute mass accumulated in the bed, i.e., dm_{TR}/dt , where m_{TR} is the tritium mass per unit bed area. Qualitatively, Figure 6 indicates that the mean residence time is on the order of 1–10 hours. The breakthrough curve after the first stretch ($x = 2100$ m in Figure 5) is also consistent with this retention time.

4.2. Evaluation of ASP Model Parameters and Model Bias Using Temporal Moments

[33] Following the procedure for modeling hyporheic exchange described in Appendix A, we will fit the ASP-model prediction to the observed solute breakthrough curves and then evaluate the ability of the model to represent the observed transport. The exchange parameters are determined by fitting the model prediction to the change of the central temporal moments of the breakthrough curve between measuring stations, (12)–(15), and the breakthrough curves are reproduced using a numerical Laplace inversion routine. The optimal residence time PDF will also be compared with the PDFs obtained from (1) bed pore water analyses and (2) pumping exchange theory.

[34] Fitting of the central temporal moments of the residence time PDF takes into account only the shape of the breakthrough curve, and not the magnitude of the in-stream concentrations. That

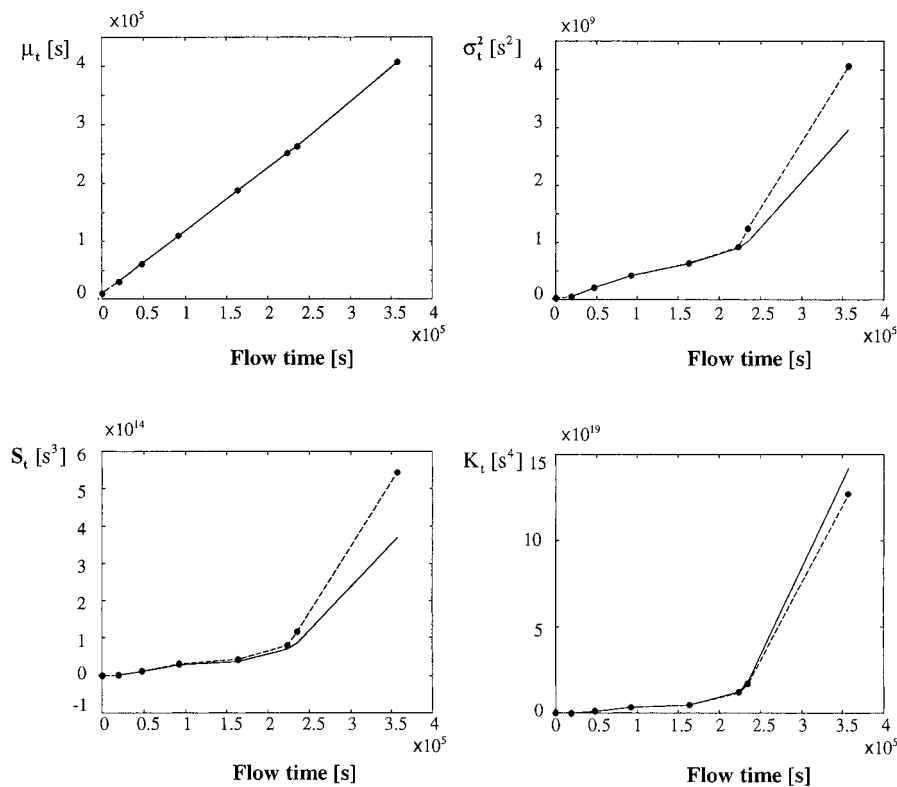


Figure 7. Central temporal moments of the tritium breakthrough curve at the eight stations along Säva Brook. Data are presented as dashed lines and circles, and the model curves are solid lines. The flow time is defined as L/U_{es} , where L is the total travel distance. The exponential T-PDF was used to derive these diagrams; thus these curves are equivalent to the fit of the Transient Storage Model to the experimental data.

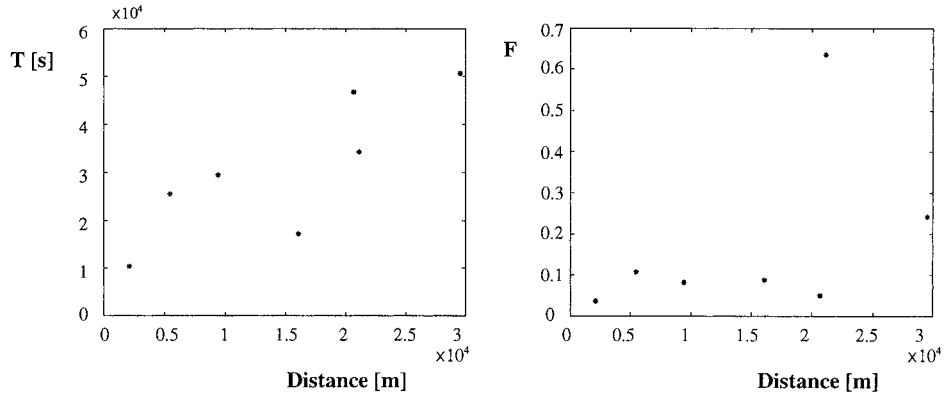


Figure 8. Variation of the residence time in the hyporheic zone, T , and hydro-mechanical retardation factor F with distance in Säva Brook. The parameter values are derived from a precise match of the first three central temporal moments. The parameters are evaluated from tritium data and indicate a high degree of water retention (high F factor) due to emergent macrophytes in stretch six.

is, the moment method analysis works on the basis of normalized breakthrough curves and is not affected by dilution. There are three unknowns for tritium transport, Q/A_T , F , and T , which means that the first three moment equations form an exactly determined system with respect to these unknowns. A formal optimization of the parameters requires that we minimize the change in the first four central temporal moments between monitoring stations:

$$\hat{\theta} = \arg \min_{\theta} \left\{ [\mathbf{Y} - \mathbf{B}(\theta)]^T [\mathbf{Y} - \mathbf{B}(\theta)] \right\}, \quad (16)$$

where $\hat{\theta}$ is the optimum estimate of the vector $\theta = [U_e; T; F]$ that minimizes the least squares sum of the argument of (16), for tritium, $\mathbf{Y} = [1; 1; 1; 1]$, $\mathbf{B} = [\delta(\mu_t)_{\text{th}}/\delta(\mu_t)_{\text{obs}}; \delta(\sigma_t^2)_{\text{th}}/\delta(\sigma_t^2)_{\text{obs}}; \delta(S_t)_{\text{th}}/\delta(S_t)_{\text{obs}}; \delta(K_t)_{\text{th}}/\delta(K_t)_{\text{obs}}]$, the δ operator denotes a change, and the subscripts “th” and “obs” denote theory and observations, respectively. The error ε is defined by the minimum of $[\mathbf{Y} - \mathbf{B}(\theta)]^T [\mathbf{Y} - \mathbf{B}(\theta)]$.

[35] Figure 7 shows how the ASP model can be fitted to the tritium data obtained from the Säva Brook Experiment 1998 using the exponential T-PDF. Recall that the exponential T-PDF is equivalent to the Transient Storage Model, so Figure 7 represents an alternate way to show the fit of the TSM to the experimental data. Table 2 lists parameter values obtained by means of the optimization given in equation (16). Since the change in the moments is reconstructed as a stepwise summation with distance in Figure 7, the discrepancy between the model and the observed values tends to increase with distance.

[36] If all exchange parameters had constant values everywhere in the stream, the first three moments should vary linearly with distance according to (12)–(14). The curves in Figure 7 are clearly nonlinear, which results from the increasing values of T and F with distance (Figure 8) and the decreasing value of U_e with distance (Table 2). The point in Figure 8 with the highest F value represents a short reach (486 m) that was heavily vegetated by emergent

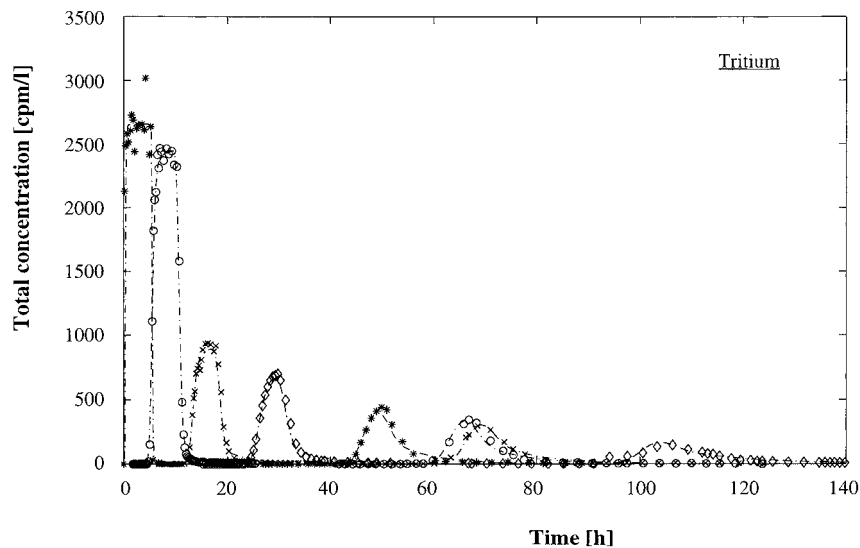


Figure 9. Breakthrough curves of $^3\text{H}_2\text{O}$ from the Säva Brook Experiment 1998 (markers) and theoretical curves produced with the ASP model (dashed lines). Parameter values used to model the tritium breakthrough were taken from the optimization based on the moment method using the exponential T-PDF (Table 2) (data after Jonsson et al. (submitted manuscript, 2001)).

macrophytes (mainly reed and cattail). This result indicates a higher accumulation capacity for solutes in such macrophyte patches, longer travel paths, and relatively high flow velocities in the hyporheic or littoral zones. However, the methods employed here cannot distinguish solute retention due to slow surface-water flow through macrophyte patches in the littoral zone or “dead zones” from actual hyporheic exchange in this reach.

[37] Figure 9 shows the breakthrough curves calculated from the exponential T-PDF using optimized parameter values. Again, this is equivalent to fitting the breakthrough curves using the Transient Storage Model. Here we have assigned a plausible value to the dispersion coefficient ($E = 0.8 \text{ m}^2 \text{ s}^{-1}$), and this has only a minor effect on the solute breakthrough curves relative to transient storage [Wörman, 2000]. The parameter values found by fitting the central temporal moments provide a good representation of the entire breakthrough curve. We can see that the fit using the exponential T-PDF is relatively good, but it can be improved by use of more realistic T-PDFs. Since the lognormal T-PDF includes two degrees of freedom, the four moment equations are not sufficient to find an optimal set of exchange parameters.

[38] The average model bias ϵ for all stations associated with different T-PDFs varies only in a small range of 14% up to 17%. The lowest bias was obtained for the Dirac delta distribution despite the fact that this representation of the exchange gives rise to the multiple peaks as shown in Figure 5. Analyses by Wörman [2000] suggest that the difference in bias between an “acceptable” and a “non-acceptable” model is much larger than we found for the T-PDFs tested here. Thus, surprisingly, any of the T-PDFs described in Table 1 can be considered to do an adequate job of representing the first four temporal moments of the breakthrough curves.

4.3. Evaluation of ASP Model Parameters From Bed Pore Water Samples

[39] Typically, field evaluations of stream-subsurface exchange would rely only on the in-stream solute breakthrough curves. The

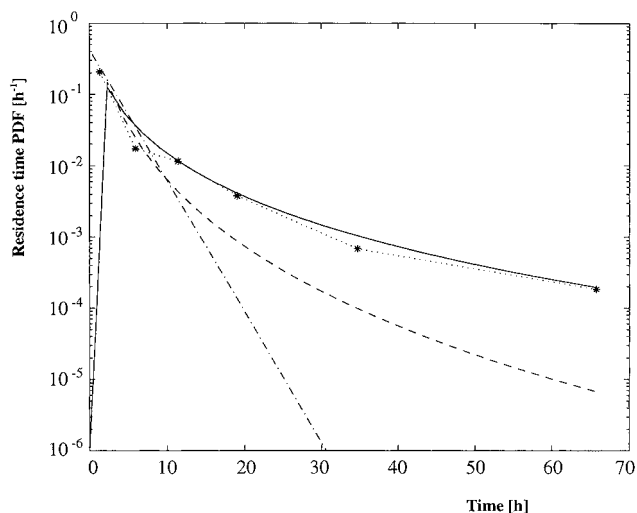


Figure 10. Residence time PDF evaluated from sediment samples taken in the Säva Brook 1998 Experiment (star markers and dotted line). The dashed-dotted line is the exponential PDF, the dashed curve is the lognormal PDF with same mean value as the data, and the solid curve is the best fit of the lognormal PDF within the time interval of the observations. The expected residence time was $\langle T \rangle = 2.36$ hours, and the corresponding values of α and β were 0.3 and 1.058 for the dashed curve and 0.7 and 1.4 for the solid curve (in units of hours).

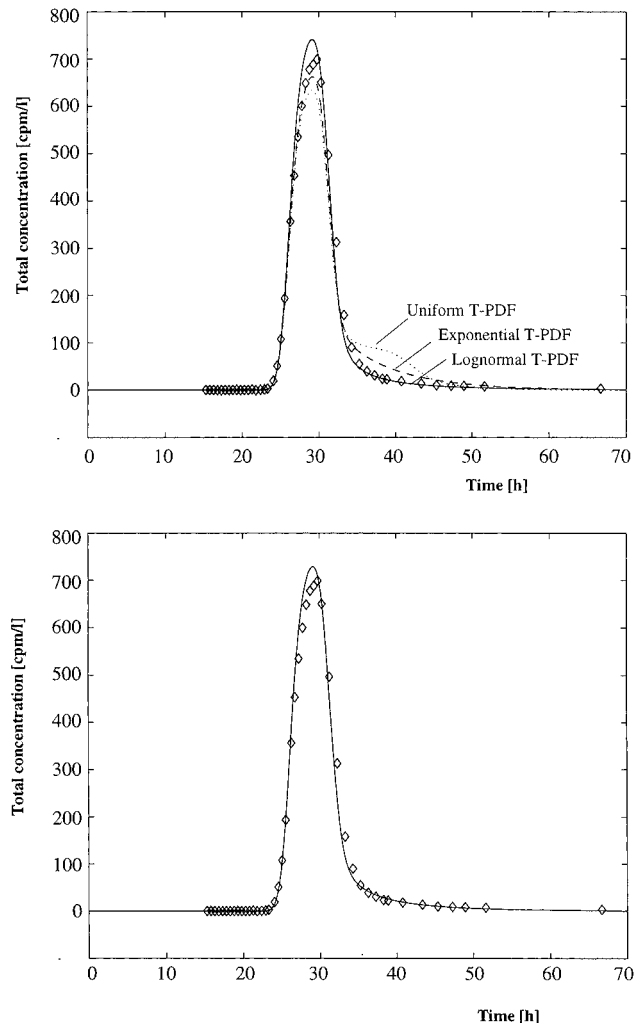


Figure 11. Breakthrough curves for $^3\text{H}_2\text{O}$. Data from the Säva Brook Experiment 1998 are open symbols. (top) Theoretical curves for the ASP model using three different T-PDFs with optimized parameters (Table 2). (bottom) Optimal fit using a combined PDF, 15% exponential and 85% lognormal.

data set of Jonsson et al. (submitted manuscript, 2001) also includes measurements of the residence time of solutes in the streambed, which allows us to evaluate the ability of the ASP model to reproduce both surface and subsurface solute transport. Figure 10 shows the exponential and the lognormal residence time PDFs fitted to the observed retention of tritium in the streambed based on the sediments samples taken at $x = 125$ m in the Säva Brook 1998 experiments. The experimental data in Figure 10 were determined by calculating $dm_{\text{TR}}(t)/dt$ from the data in Figure 6 and assuming that the change in the mass flux is zero after 100 hours.

[40] The expected value of the residence time obtained from this evaluation was ~ 8.506 s (2.36 hours), which correlates well with the residence times found by optimizing the central temporal moments to the in-stream data (Figure 8 and Table 2). We can see in Figure 10 that the lognormal function fits the observations better than the exponential function, especially at the longer residence times. As the theoretical probability density functions are infinite and the observed PDF is taken to be limited at 66 hours (where it drops to zero), the infinite functions fall somewhat below the observed values if they are forced to have the same mean value (dashed and dashed-dotted curves). However, the deviation for the

best fitted lognormal PDF with a mean value of 2.36 hours (dashed curve) is relatively small; after 60 hours, it is only $\sim 10^{-4}$ or one per mille of the peak value. The best fit in the observed time interval is obtained for $\alpha = 0.7$ and $\beta = 1.4$ (solid curve) which yields about twice the observed mean value.

[41] According to the pumping exchange model with homogeneous hydraulic conductivity, the value of β increases from about 0.95 when the relative depth of the hyporheic zone $d_b/\lambda = 0.25$ up to 1.9 when $d_b/\lambda > 1$ (in both cases $\alpha \approx 1.35$). The fact that these values delimit the experimentally determined value of β (1.05–1.4) may indicate a limitation of the hyporheic zone, e.g., due to decreasing hydraulic conductivity (porosity) with depth. Measurements indicate a consistently lower hydraulic conductivity at the 7-th than at the 3-cm-depth.

[42] At shorter times the exponential T-PDF provides a very good fit, and this is probably due to the fact that the wave crests of the uneven bed yields additional short travel paths. Marion et al. (submitted manuscript, 2001) observed a similar behavior in a laboratory flume study. Since the exponential distribution exactly represents a first-order mass transfer relationship, we can expect the Transient Storage Model to be a good approximation of the actual transient storage processes, particularly at the shorter times typically observed in tracer studies.

[43] For analysis of transport over timescales of days or longer, we expect that the exponential approximation would no longer be sufficient and an accurate representation of the residence time of solutes in the hyporheic zone would be required. One way that this can be accomplished is to add different types of PDFs to represent the entire range of relevant timescales. The suggestion of Choi et al. [2000] that multiple Transient Storage parameters be used to represent exchange would also allow the observed curves to be reproduced. However, it should be emphasized again that the first-order mass transfer approximation of the TSM is not physically based, and thus lacks generality. The use of multiple TSM exchange coefficients is simply equivalent to fitting observed solute breakthrough curves with multiple exponential functions. We suggest that it would be preferable to construct a model using different physically based T-PDFs, which represent different exchange mechanisms and can be parameterized to allow generalization to different streamflow conditions.

[44] The use of various T-PDF solutions will be demonstrated by retaining the optimized parameter values and using one particular breakthrough curve as an example. Both the exponential and the lognormal T-PDF provide acceptable representations of the breakthrough curve measured at $x = 5434$ m in Säva Brook, as shown in the left-hand graph in Figure 11. The uniform residence time distribution did not work as well, as it underestimated the peak concentration and produced an unrealistic shape of the tail. The tail of the breakthrough curve is best described by the lognormal distribution, whereas a combination of lognormal and exponential functions gives the optimal fit, as shown in the right-hand graph in Figure 11. Multiple exponentials could have been used to fit the tail as well. Overall, the difference in model fit due to the different T-PDFs is small and is further obscured by uncertainty on the order of 5% due to the effect of dilution.

5. Equating Exchange Coefficients With State Variables of the Stream

[45] In this study we found strong indications that the uptake of solutes in streambeds is driven by advection induced by pressure variations at the bed surface. In other studies the residence time of

solute in the hyporheic zone has been found to vary between 5 and 295,000 s [Czernuszenko et al., 1998; Harvey and Fuller, 1998; Wörman, 2000; Seo and Cheong, 2001; Fernald et al., 2001]. Here we have found residence times in the range of 10,000–50,000 s, as shown in Figure 7. The wide range of observed residence times suggests that different processes control the exchange in different reaches and that there could be a successive change in the storage processes in streams of different size and character.

[46] This section will use the hydro-mechanical principles introduced in section 2.2 to express the residence time for solutes in the hyporheic zone (or α_{st}) in terms of state variables of the stream. The principles of section 2.2 will be applied to the exchange due to the pressure variation caused by the uneven bed surface. Even though the actual stream geometry differs slightly from the idealization employed in developing the exchange model, the results from section 4 indicate that the pumping exchange model provides an acceptable interpretative model framework for Säva Brook.

[47] If we combine (3) and (11) and substitute $A = bh$ and $A_s = bd_b$, where b is the surface width of the stream, $h = A/b$ is the hydraulic mean depth of the stream, and $d_b = A_s/b$ is the mean depth of the hyporheic zone, we can derive an expression for the exchange rate coefficient α_{st} :

$$\alpha_{st} = 4/21 \pi^2 \frac{h_m K}{\lambda h}. \quad (17)$$

This equation is only valid when $d_b/\lambda \leq 1$. We can see from (3), (4), and (17) that many of the relevant properties reflecting the transient storage are governed by the ratio between the pressure head and wavelength (h_m/λ). The pressure head that drives the pumping exchange (Figure 1) can be calculated from the following approximate relationship proposed by Elliott [1990] based on the data of Fehlman [1985]:

$$h_m = 0.28 \left(\frac{H/h}{0.34} \right)^r \frac{U^2}{2g}, \quad (18)$$

where H is the bed form height (m) and r is a coefficient that takes the value 3/8 for $H/h \leq 0.34$ and 3/2 for $H/h \geq 0.34$. Substituting (18) into (17) yields the following relationship:

$$\alpha_{st} = \frac{2\pi^2}{21} C_1 Fr^2 \frac{h}{\lambda} K \quad (19)$$

where the Froude number $Fr = U/(gh)^{0.5}$ and the coefficient $C_1 = 0.28 [(H/h)/0.34]^r$ is a geometric factor based on the relative penetration of bed forms in the stream. Both the Froude number dependence and the geometric coefficient C_1 result from the fact that form drag over bed forms drives the pumping process. In the Säva experiment we found that almost all of the solutes accumulated in the surficial part of the alluvial sediment, where the pumping exchange is assumed to occur (>95% of the mass was accounted for in the upper 21 cm of the sediment bed).

[48] In terms of residence time, the dimensionless residence time due to pumping exchange can be expressed by combining (11) with (19)

$$\frac{\langle T \rangle K}{h} = \frac{21}{2\pi^2 C_1} \frac{d_b \lambda}{h^2} \frac{1}{Fr^2}. \quad (20)$$

The corresponding relationship for the exchange velocity (based on equation (4)) is $\langle V_z \rangle_{z=0} K = C_1 \pi (h/\lambda) Fr^2$. These sorts of

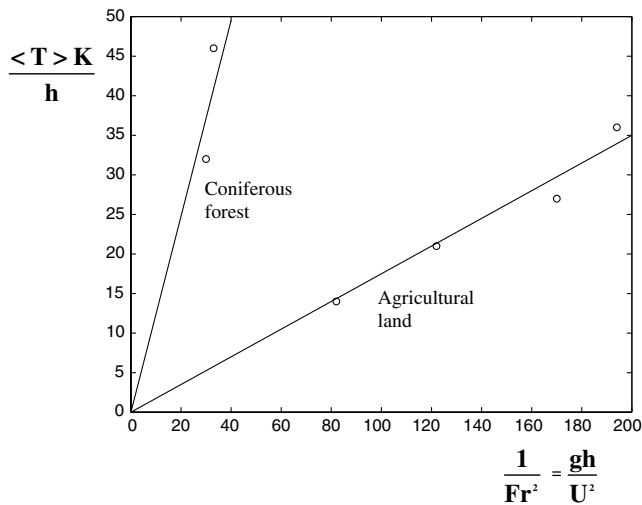


Figure 12. Evaluation of the effect of land use or stream morphology on hyporheic exchange, evaluated from the Säva Brook Experiment 1998. The solid lines represent the trends between the dimensionless time and the stream Froude number expected from pumping exchange theory. The theory has been fit to the data by adjusting the unknown variable $(\lambda d_b)/(C_1 h^2)$, which is the slope of the curves on this dimensionless plot.

representations are very useful because they explicitly consider the effects of channel geometry and flow velocity on stream-subsurface exchange. In particular, consideration of the mechanisms of hyporheic exchange allows experimental results to be generalized to different streamflow conditions. In addition, equation (20) can be used to analyze the factors that produce reach-to-reach variations in hyporheic exchange *independently* from variations in streamflow and channel geometry.

[49] If we consider the lumped parameter $(\lambda d_b)/(C_1 h^2)$ as an unknown proportionality coefficient for Säva Brook, then this parameter can be found from the experimental data by plotting the dimensionless time $\langle T \rangle K/h$ against the Froude number $U/(gh)^{0.5}$ as shown in Figure 12. The data obtained for the dense macrophyte patch between 20,633 and 21,119 m are excluded from Figure 12 because of difficulties of defining the geometric properties in this part of the brook. As can be seen from (20) and Figure 12, the mean residence time increases with decreasing Froude number. The hydraulic conductivity and the stream depth scale the residence time.

[50] The trend of the results from the first two stretches of Säva Brook deviates from the trend of the remaining stretches. This difference is presumably due to variations in hyporheic exchange in these reaches as reflected in the parameter grouping $(\lambda d_b)/(C_1 h^2)$, which is the slope of the dimensionless curves in Figure 12. Unfortunately, we do not have data for the relative bed form height, H/h , relative bed form wavelength, λ/h , or relative depth of the alluvial bed, d_b/h . However, qualitative observations of the stream geomorphology in the forested and agricultural regions support the idea that $(\lambda d_b)/(C_1 h^2)$ varied with land use in Säva Brook.

[51] The first two stretches of the brook flow through coniferous forest, and the stream contains organic-rich sediments and debris such as tree branches and boulders. The remaining part of Säva Brook flows through agricultural land, and the channel has emergent macrophytes instead of loose debris. In this agricultural land, Säva Brook meanders in some places but has partly been converted to an excavated drainage ditch. It is apparent that some

factor related to land use, such as channel morphology or sediment composition, controls the hyporheic exchange in the various reaches of Säva Brook. The proportionality coefficients $(\lambda d_b)/(C_1 h^2)$ for the two land use types are ~ 1.2 and ~ 0.2 , respectively, as found from the slopes of the curve fits in Figure 12.

6. Conclusions

[52] The pressure variation associated with an uneven streambed surface leads to an induced flow of water and solutes between the stream and the hyporheic zone. From this study it appears that the pumping exchange model proposed by *Elliott and Brooks* [1997a] and *Packman et al.* [2000a] provides a reasonable approximation for the hyporheic exchange occurring in Säva Brook, Sweden. By including flow-induced hyporheic exchange in a model for longitudinal transport of solutes in streams, here denoted the ASP model, we were able to explain the observed solute transport that occurred following a tracer injection of $^3\text{H}_2\text{O}$ in Säva Brook.

[53] By expressing in closed form the central temporal moments for solute breakthrough in the stream, equations (12)–(15), we assessed the effect of different residence time PDFs in the hyporheic zone on the mean, as well as higher-order moments, of the solute residence times in the stream. The ASP model with an exponential residence time PDF yields breakthrough curves that are identical to those produced by the Transient Storage Model, where hyporheic exchange is expressed as a first-order mass transfer. However, advective pumping exchange was found to be best represented by a lognormal residence time distribution.

[54] While all residence time functions tested produced adequate representations of the observed solute transport in the main stream, the lognormal PDF provided the best representation of the observed breakthrough curves. From a large number of samples of bottom sediments in Säva Brook, the residence time distribution of solute in the storage zone was also found to be best represented by a lognormal PDF. The expected value of the residence times evaluated from the pore water inventory correlates well with the value obtained from analysis of in-stream concentrations. Furthermore, the pumping model explained the spatial variation of the hyporheic exchange along Säva Brook in terms of a variation of the stream morphology and flow rate. Thus we conclude that advective pumping flows dominated the hyporheic exchange in Säva Brook.

[55] Because it is physically based, the hydrodynamic pumping exchange model can be used to generalize the experimental results. This represents a considerable advantage relative to current empirical exchange models, which cannot easily be generalized. On the basis of the premise that pumping exchange caused by bed roughness dominated the transient storage in the Säva Brook experiment, approximate constitutive relationships were derived that relate the expected residence time and exchange velocity or exchange rate of the Transient Storage Model with stream properties. Exchange was parameterized to relate the dimensionless hyporheic residence time (timescale is the ratio of stream size and hydraulic conductivity of bed sediments) with the stream Froude number. Both theory and observations indicate that the exchange rate increases and the residence time decreases with Froude number. This parameterization allows consideration of hyporheic exchange in different stream reaches independently from variations in streamflow and channel geometry. This approach was successfully used to distinguish hyporheic exchange in sections of Säva Brook with different land use.

Appendix A: Methods of Solution for ASP Model

[56] All parameters except discharge are assumed to be constants along subreaches of the stream. The volumetric flow rate, $Q = UA$, is assumed to vary linearly along each subreach according to $Q/Q_0 = (1 + \theta x)$, where Q_0 is the upstream flow rate, Q is the downstream flow rate, and θ is a proportionality coefficient. For such a discharge variation, Forsman [2000] showed that the problem could readily be solved in the Laplace domain following similar steps as those of Maloszewski and Zuber [1990].

[57] On the assumption that there is a symmetric flow field in the sediment bed, the variation of A_i and V_z along the travel path is not important to the concentration at the end of the path (i.e., at $\tau = T$). Hence the solution to (5) and (6) becomes $\bar{g}_d = \bar{c}_d(x) \exp(-s\tau)$, where a Laplace transform of an arbitrary function uis defined as $\bar{u} = \int_0^\infty ue^{-st} dt$, s is an arbitrary real number, and $\tau = z/(V_z/n)$. This gives us the source/sink expressed by (1) in a simple manner that allows inclusion of additional diagenetic processes if required. Provided a unit Dirac pulse at the upstream boundary, zero initial concentration elsewhere ($g_d(t=0) = c_d(t=0) = 0$), and an infinite stream, the solution \bar{S}_D to (1) and (2) becomes

$$\bar{S}_D = \frac{\bar{c}_T}{M/Q} = (1 + \theta x)^{-1} \exp \left[\left(\frac{Q}{2EA_T} - \sqrt{\left(\frac{Q}{2EA_T} \right)^2 + \frac{s}{E} - \left\langle \frac{1}{2} \xi \frac{PV_z}{AE} (e^{-sT} - 1) \right\rangle} \right) x \right], \quad (A1)$$

where M is the total solute mass injected at $x = 0$. Since the transports along each travel path in the hyporheic zone are assumed to be independent, the averaging $\langle \dots \rangle$ reflected by the integral in (1) is readily performed for any known form of $f(T)$ after the derivation of (A1).

[58] The real-domain solution S_D (s^{-1} is found means of the series expansion method of De Hoog *et al.* [1982] using a numerical algorithm by K.J. Hollenbeck (INVLAP.M: A Matlab function for numerical inversion of Laplace transforms by the De Hoog algorithm, available at <http://www.isva.dtu.dk/staff/karl/invlap.htm>, 1998). Since S_D is the solution at a section x due to a unit Dirac pulse introduced at the boundary, the concentration at a section x for a temporal variation of the boundary concentration, G_{BC} (kg m^{-3}), is given by the following convolution operation (compare textbook on mathematical methods of physics):

$$G_x(t) = \int_0^t S_D(t - \tau) G_{BC}(\tau) d\tau. \quad (A2)$$

If the Peclet number $(ux)/E$ is sufficiently large (as it often is), we can use the solution as a boundary condition for the next downstream reach. Hence we can stepwise find the solution for a set of subreaches by substituting $G_{BC} = G_x$ before we use (A2) to calculate a new G_x for the next reach.

[59] Further, since the Laplace transform is a moment-generating function, we can easily derive the temporal moments of the breakthrough curve by repeated derivation of (A2) with respect to s and evaluating the result for $s = 0$ [Wörman, 2000]. Similar techniques have been applied previously to solute transport in stream by Nordin and Troutman [1980], Schmid [1995], Schmid [1997] and Czernuszenko and Rowinski [1997].

A.1. Notation

- A cross-sectional area of the main stream excluding stagnant side pockets [m^2].
- A_T cross-sectional area of the stream including stagnant side pockets [m^2].
- A_s storage area of hyporheic zone [m^2].
- b surface width of stream [m].
- a, b, c constants in the expressions of central temporal moments.
- c solute mass per unit volume of water in main stream channel [kg m^{-3}].
- C_1 coefficient in pumping theory.
- d (subscript) “dissolved”.
- d_b depth of hyporheic zone [m].
- E dispersion coefficient [$\text{m}^2 \text{s}^{-1}$].
- F retardation factor for the solute transport [].
- Fr Froude number, equal to $U/(gh)^{0.5}$ [].
- f probability density function for residence time in the hyporheic zone [h^{-1}], [s^{-1}].
- g solute mass per unit volume of water in the hyporheic zone [kg m^{-3}], acceleration due to gravity [m s^{-2}].
- G solution to (1)–(5).
- h hydraulic mean depth of the stream (area divided by surface width) [m].
- h_m maximum deviation in pressure head [m].
- H bed form height [m].
- J_s exchange rate of solute mass per unit cross-sectional area of stream [$\text{kg m}^{-2} \text{s}^{-1}$].
- K_t kurtosis of residence time [t^4].
- K hydraulic conductivity [m s^{-1}].
- M total solute mass [kg].
- n porosity [].
- P wetted perimeter [m].
- Q water discharge in stream [$\text{m}^3 \text{s}^{-1}$].
- R_h A/P , equal to hydraulic radius [m].
- S_t skewness of residence time [t^3].
- S_D solution to (1)–(5) provided a unit Dirac pulse at the upstream boundary.
- T total residence time from inlet to exit of hyporheic flow path [s].
- $T^* = 4 \pi^2 \langle T \rangle Kh_m / \lambda^2$.
- t time [s].
- U flow velocity in the main stream channel [m s^{-1}].
- $U_e = Q/A_T$ [m s^{-1}].
- $u_{adv}^* = (u_{adv} \lambda) / (2 \pi Kh_m)$.
- V_z infiltration or exfiltration Darcy water velocity, equal to pore velocity \times porosity [m s^{-1}].
- V_n velocity component perpendicular to the bed [m s^{-1}].
- $V_z^* = (V_z \lambda) / (2 \pi Kh_m)$.
- X length of stream associated with one wave length [m].
- x curve-linear longitudinal coordinate along stream [m].
- z curve-linear coordinate along hyporheic flow path.
- α_{sr} exchange rate coefficient defined by a first-order mass transfer relationship [s^{-1}].
- Δ duration of pulse at upstream boundary [s].
- δ operator representing a difference.
- $\delta(t)$ Dirac delta function [].
- ε relative error [].
- μ_t expected value of residence time = $E[t]$ [s].
- θ dilution parameter.

- λ wavelength of pressure variations along bed [m].
 σ^2 variance of residence time [t^2].
 τ residence time along hyporheic flow path [s].
 ξ area reduction factor, equal to $\int_0^\infty V_n/V_z f(T) dT$ []

[60] **Acknowledgments.** This study was supported by a research program initiated by the Swedish National Energy Administration. Aaron Packman's involvement in this study was supported by NSF CAREER award BES-0196368. The authors are grateful for the help of Göran Reh binder in evaluating the slug tests. Three anonymous reviewers provided constructive comments that helped improve this paper.

References

- Bencala, K. E., and R. A. Walters, Simulation of solute transport in a mountain pool-and-riffle stream: a transient storage model, *Water Resour. Res.*, 19(3), 718–724, 1983.
- Castro, N. M., and G. H. Hornberger, Surface-subsurface water interactions in an alluviated mountain stream channel, *Water Resour. Res.*, 27(7), 1613–1621, 1991.
- Choi, J., J. W. Harvey, and M. H. Conklin, Characterizing multiple timescales and storage zone interaction that affect solute fate and transport in drainage basins, *Water Resour. Res.*, 36(6), 1511–1518, 2000.
- Comans, R. N. J., and D. E. Hockley, Kinetics of cesium sorption on illite, *Geochem. Cosmochim. Acta*, 56, 1157–1164, 1992.
- Czernuszenko, W., and P. M. Rowinski, Properties of the dead-zone model of longitudinal dispersion in rivers, *J. Hydraul. Res.*, 35(4), 491–504, 1997.
- Czernuszenko, W., P.-M. Rowinski, and A. Sukhodolov, Experimental and numerical validation for longitudinal dispersion in rivers, *J. Hydraul. Res.*, 36(2), 269–280, 1998.
- De Hoog, F. R., J. H. Knight, and A. N. Stokes, An improved method for numerical inversion of Laplace transforms, *J. Sci. Stat. Comput.*, 3(3), 357–366, 1982.
- Elliott, A. H., Transport of solutes into and out of stream beds, Ph.D. thesis, W. M. Keck Lab. of Hydraul. and Water Resour., Calif. Inst. of Technol., Pasadena, 1990.
- Elliott, A. H., and N. H. Brooks, Transfer of nonsorbing solutes to a streambed with bed forms: Theory, *Water Resour. Res.*, 33(1), 123–136, 1997a.
- Elliott, A. H., and N. H. Brooks, Transfer of nonsorbing solutes to a streambed with bed forms: Laboratory experiments, *Water Resour. Res.*, 33(1), 137–151, 1997b.
- Eylers, H., N. H. Brooks, and J. J. Morgan, Transport of adsorbing metals from stream water to a stationary sand-bed in a laboratory flume, *Mar. Freshwater Res.*, 46, 209–214, 1995.
- Fehlman, H. M., Resistance components and velocity distribution of open channel flows over bed forms, M.S. thesis, Colo. State Univ., Fort Collins, 1985.
- Fernald, G. A., P. J. Wington, and D. H. Landers, Transient storage and hyporheic flow along the Willamette River, Oregon: Field measurements and model estimates, *Water Resour. Res.*, 37(6), 1681–1694, 2001.
- Forsman, J., Contaminant transport in non-uniform streams and streambeds, Ph.D. thesis, Uppsala Univ., Uppsala, Sweden, 2000.
- Freeze, R. A., and J. A. Cherry, *Groundwater*, Prentice-Hall, Englewood Cliffs, N. J., 1979.
- Harvey, J., and K. E. Bencala, Effect of streambed topography on surface-subsurface water exchange in mountain catchments, *Water Resour. Res.*, 29(1), 89–98, 1993.
- Harvey, J. W., and C. C. Fuller, Effect of enhanced manganese oxidation in the hyporheic zone on basin-scale geochemical mass balance, *Water Resour. Res.*, 34(4), 623–636, 1998.
- Harvey, J. W., B. J. Wagner, and K. E. Bencala, Evaluating the reliability of the stream tracer approach to characterize stream-subsurface water exchange, *Water Resour. Res.*, 32(8), 2441–2451, 1996.
- Huettel, M., W. Ziebis, and S. Forster, Flow-induced uptake of particulate matter in permeable sediments, *Limnol. Oceanogr.*, 41(2), 309–322, 1996.
- Hutchinson, P. A., and I. T. Webster, Solute uptake in aquatic sediments due to current-obstacle interactions, *J. Environ. Eng.*, 124(5), 419–426, 1998.
- Jackman, A. P., R. A. Walters, and V. C. Kennedy, Transport and concentration controls for chloride, strontium, potassium and lead in Uvas Creek, a small cobble-bed stream in Santa Clara County, California, USA, *J. Hydrol.*, 75, 67–141, 1984.
- Johansson, H., K. Jonsson, J. Forsman, and A. Wörman, Retention of conservative and sorptive solutes in rivers-simultaneous tracer experiments, *Sci. Total Environ.*, 266(2001), 229–238, 2000.
- Jonsson, K., and A. Wörman, Effect of sorption kinetics on the transport of solutes in streams, *Sci. Total Environ.*, 266(2001), 239–247, 2000.
- Kim, B. K. A., A. P. Jackman, and F. J. Triska, Modeling biotic uptake by periphyton and transient hyporheic storage of nitrate in a natural stream, *Water Resour. Res.*, 28(19), 2743–2752, 1992.
- Maloszewski, P., and A. Zuber, Mathematical modelling of tracer behavior in short-term experiments in fissured rocks, *Water Resour. Res.*, 26(7), 1517–1528, 1990.
- Meili, M., and A. Wörman, Desorption and diffusion of episodic pollutants in sediments: A 3-phase model applied to Chernobyl 137Cs, *Appl. Geochem.*, 11, 311–316, 1996.
- Nordin, C. F., and B. M. Troutman, Longitudinal dispersion in rivers: The persistence of skewness in observed data, *Water Resour. Res.*, 16(1), 123–128, 1980.
- Onishi, Y., Sediment-contaminant transport model, *J. Hydraul. Div. Am. Soc. Civ. Eng.*, 107(HY9), 1089–1107, 1981.
- Packman, A. I., Scaling bedform-driven exchange between a stream and a finite stream bed, paper presented at 28th International Association for Hydraulic Research Congress, Graz, Austria, Aug. 1999.
- Packman, A. I., and K. Bencala, Modelling surface-subsurface hydrological interconnections, in *Streams and Groundwaters*, edited by J. B. Jones, and P. J. Mulholland, pp. 45–80, Academic, San Diego, Calif., 1999.
- Packman, A. I., and N. H. Brooks, Hyporheic exchange of solutes and colloids with moving bed forms, *Water Resour. Res.*, 37(10), 2591–2605, 2001.
- Packman, A. I., N. H. Brooks, and J. J. Morgan, Experimental techniques for laboratory investigation of clay colloid transport and filtration in a stream with a sand bed, *Water Air Soil Pollut.*, 99(1–4), 113–122, 1997.
- Packman, A. I., N. H. Brooks, and J. J. Morgan, A physicochemical model for colloid exchange between a stream and a sand streambed with bed forms, *Water Resour. Res.*, 36(8), 2351–2361, 2000a.
- Packman, A. I., N. H. Brooks, and J. J. Morgan, Kaolinite exchange between a stream and streambed: Laboratory experiments and validation of a colloid transport model, *Water Resour. Res.*, 36(8), 2363–2372, 2000b.
- Raudkivi, A., *Loose Boundary Hydraulics*, 2nd ed., Pergamon, New York, 1998.
- Richardson, C. P., and A. D. Parr, Modified Fickian model for solute uptake by runoff, *J. Environ. Eng.*, 144(4), 792–809, 1988.
- Runkel, R. L., and K. E. Bencala, Transport of reacting solutes in rivers and streams, in *Environmental Hydrology*, edited by V. P. Singh, pp. 137–164, Kluwer Acad., Norwell, Mass., 1995.
- Runkel, R. L., K. E. Bencala, R. E. Broshers, and S. C. Chapra, Reactive solute transport in streams, 1, Development of an equilibrium-based model, *Water Resour. Res.*, 32(2), 409–418, 1996a.
- Runkel, R. L., K. E. Bencala, R. E. Broshers, and S. C. Chapra, Reactive solute transport in streams, 2, Simulation of a pH modification experiment, *Water Resour. Res.*, 32(2), 419–430, 1996b.
- Rutherford, J. C., G. J. Latimer, and R. K. Smith, Bedform mobility and benthic oxygen uptake, *Water Res.*, 27(10), 1545–1558, 1993.
- Rutherford, J. C., J. D. Boyle, A. H. Elliott, T. V. J. Hatherell, and T. W. Chiu, Modeling benthic oxygen uptake by pumping, *J. Environ. Eng.*, 21(1), 84–95, 1995.
- Salomons, W., and U. Förstner, *Metals in the Hydrocycle*, Springer-Verlag, New York, 1984.
- Schmid, B. H., On the transient storage equations for longitudinal solute transport in open channels: Temporal moments accounting for the effect of first-order decay, *J. Hydraul. Res.*, 33(5), 595–610, 1995.
- Schmid, B. H., Analytical solution of the transient storage equations accounting for solute decay, paper presented at 27th International Association for Hydraulic Research Congress, San Francisco, Calif., 1997.
- Seo, I. W., and T. S. Cheong, Moment-based calculation of parameters for the storage zone model for river dispersion, *J. Hydraul. Eng.*, 127(6), 453–465, 2001.
- Smith, J. T., and R. N. J. Comans, Modelling the diffusive transport and remobilisation of ^{137}Cs in sediments: The effect of sorption kinetics and reversibility, *Geochem. Cosmochim. Acta*, 60, 995–1004, 1996.
- Thackston, E. L., and K. B. Schnelle, Predicting effects of dead-zones on stream mixing, *J. Sanit. Eng. Div. Proc. Am. Soc. Civ. Eng.*, 96, 319–331, 1970.
- Thibodeaux, L. J., and J. D. Boyle, Bedform-generated convective-transport in bottom sediments, *Nature*, 325(6102), 341–343, 1987.
- Vanoni, V. A. (Ed.), *Sedimentation engineering, ASCE Manuals Rep. Eng. Pract.* 54, Am. Soc. of Civ. Eng., New York, 1975.

- Wood, T. M., and A. M. Baptista, A model for diagnostic analysis of estuarine geochemistry, *Water Resour. Res.*, 29(1), 51–71, 1993.
- Wörman, A., Analytical solution and timescale for transport of reactive solutes in rivers and streams, *Water Resour. Res.*, 34(10), 2703–2716, 1998.
- Wörman, A., Comparison of models for transient storage in small streams, *Water Resour. Res.*, 36(2), 455–468, 2000.
- Wörman, A., J. Forsman, and H. Johansson, Modelling retention of sorbing solutes in streams based on a tracer experiment using ^{51}Cr , *J. Environ. Eng.*, 124(2), 122–130, 1998.
- Wroblicky, G. J., Seasonal variation in surface-subsurface water exchange and lateral hyporheic area of two stream-aquifer systems, *Water Resour. Res.*, 34(3), 317–328, 1998.
-
- H. Johansson, K. Jonsson, and A. Wörman, Department of Earth Sciences, Uppsala University, Villavägen 16, 752 36, Uppsala, Sweden. (anders.worman@geo.uu.se)
- A. I. Packman, Department of Civil Engineering, Northwestern University, 2145 Sheridan Road, Evanston, IL 60208-3109, USA.